

Peak Apical Recoil Rate is a Simplified Index of Left Ventricular Untwist: Validation and Application for Assessment of Diastolic Function in Children

putri yubbu (✉ drputri@upm.edu.my)

Faculty of Medicine and Health Science, Universiti Putra Malaysia <https://orcid.org/0000-0001-5477-9847>

Hunter Kauffman

The Children's Hospital of Philadelphia

Renzo Calderon-Anyosa

CHOP: The Children's Hospital of Philadelphia

Andrea E. Monteroa

The Children's Hospital of Philadelphia

Tomoyuki Sato

The Children's Hospital of Philadelphia

Daisuke Matsubara

The Children's Hospital of Philadelphia

Anirban Banerjee

The Children's Hospital of Philadelphia

Research Article

Keywords: Diastolic function, peak apical recoil rate, speckle tracking echocardiography, pediatric, cardiomyopathy

Posted Date: December 8th, 2021

DOI: <https://doi.org/10.21203/rs.3.rs-1129792/v1>

License: © ⓘ This work is licensed under a Creative Commons Attribution 4.0 International License.

[Read Full License](#)

Version of Record: A version of this preprint was published at The International Journal of Cardiovascular Imaging on March 15th, 2022. See the published version at <https://doi.org/10.1007/s10554-022-02587-y>.

Abstract

Aims

To simplify measurement of untwist by measuring the recoil rate of LV apex only, to validate and apply peak apical recoil rate (PARR) as an index of diastolic dysfunction (DD) in pediatric subjects during increased and decreased lusitropic states.

Methods and Results

We recruited 153 healthy subjects (mean age 13.8 ± 2.9 years), of whom 48 performed straight leg raising exercise and an additional 46 patients (mean 8.4 ± 5.6 years) with documented pulmonary capillary wedge pressures (PCWP) (validation cohort). In addition, we studied 16 dilated cardiomyopathy patients (mean age 9.5 ± 6.3 years) (application cohort). PARR and isovolumic relaxation time (IVRT) were compared to PCWP. Both PARR and PARR normalized by heart rate (nPARR) were excellent in detecting patient with $PCWP \geq 12$ mmHg and greatly superior to IVRT in this respect (AUC: 0.98, 95% CI [0.96, 1.0] vs. AUC: 0.7 95%CI [0.54,0.86]). In DCM patients, PARR and nPARR were greatly decreased compared to controls ($-38.58 \pm 18.59^\circ/s$ vs $-63.07 \pm 16.35^\circ/s$, $p < 0.001$) and ($-0.43 \pm 0.20^\circ/s/min$ vs $-0.83 \pm 0.28^\circ/s/min$, $p < 0.0001$) but increased with straight leg raising exercise ($-59.4 \pm 19.4^\circ/s$ vs $-97.82 \pm 39.0^\circ/s$, $p < 0.01$) and (-0.85 ± 0.36 vs $-1.4 \pm 0.62^\circ/s/min$ ($p < 0.0001$)). The intra-observer and inter-observer intraclass correlation (ICC) coefficients were 0.95 and 0.88, respectively.

Conclusion

PARR successfully detected increased and decreased lusitropic states and was not affected by age when normalized with heart rate. Both PARR and nPARR are superior to IVRT in their correlation with PCWP and offer incremental value over traditional indices of DD. This highly reproducible parameter may potentially serve as a useful index of elevated PCWP in children.

Introduction

Conventional techniques for evaluating left ventricular (LV) diastolic function in adults are often imprecise in children. Dragulescu *et al.* had demonstrated that the adult diagnostic algorithms of the American Society of Echocardiography (ASE) incorrectly classified up to 30% of children having overt and often severe cardiomyopathy as having normal diastolic function, even when the adult cutoff values were replaced with pediatric reference values [1].

LV diastolic function is influenced by LV relaxation, early diastolic recoil, and myocardial stiffness, all of which determine LV filling pressures directly or indirectly [2]. LV untwisting rate is a novel index of early diastolic function that has been investigated extensively in adults as a surrogate marker for early diastolic recoil [2]. However, similar studies are infrequent in children.

The helical arrangement of LV myofibers results in a twisting motion during systole and an untwisting or recoil motion during diastole. Due to the dominant rotation of the LV apex versus the base, potential energy is stored in the apical region of the LV when it contracts (restoring force). The release of this potential energy in early diastole may be responsible for the rapid untwist phenomenon, generating enough suction that initiates LV filling [3]. At the cellular level, giant protein titin acts as an elastic spring that is compressed during systole, and its recoil during diastole plays an important role in LV expansion [4]. LV elastic recoil during isovolumic relaxation contributes to the decline in LV pressure [3]. Therefore, LV untwisting rate may serve as a useful marker in evaluating LV relaxation abnormalities. However, the measurement of untwisting by 2D echocardiography (2DE) involves evaluating both apical and basal rotations by performing off-line measurements. This may prove complicated and burdensome in busy clinical laboratories, thereby, explaining its limited use in clinical practice [2].

We have previously shown that the untwist increased substantially at the LV apex during exercise and hardly at the base [5]. This finding suggests that the apex may serve as a functional reserve for LV filling during diastole, which can be called into action during increased physical activity. Like peak untwisting rate, peak apical recoil rate (PARR) can be determined readily from a sharp inflection point, produced during early diastole, which is measurable relatively easily (Figure 1).

Therefore, the purpose of this study is to validate the use of PARR as an index of early diastolic function, with application in altered lusitropic states and to determine if PARR correlates with PCWP. We hypothesize that PARR can be used as a simplified index of LV relaxation and may provide incremental value as a noninvasive marker of DD in children.

Methodology

Study design and participants

The study consisted of two arms: a validation arm and an application arm. For the validation arm, we retrospectively enrolled patients with documented PCWP in catheterization reports. They were divided into normal mean PCWP (< 12 mm Hg) and elevated mean PCWP (≥ 12 mm Hg) groups [6]. The patients with normal PCWP mainly consisted of patients with underlying congenital or acquired heart disease, undergoing diagnostic catheterizations. The patients with elevated PCWP comprised of patients with restrictive, dilated, and hypertrophic cardiomyopathies and aortic stenosis. The median time between cardiac catheterization and echocardiogram was 16 days. All patients were in sinus rhythm. Patients with mitral stenosis or more than mild mitral regurgitation, bundle branch block, and LV dyssynchrony were excluded.

For the application arm, we prospectively enrolled healthy subjects less than 18 years old. They were enrolled from the population of children being evaluated in the echocardiography laboratory for routine indications such as chest pain, syncope, murmur, or family history of cardiomyopathy. The healthy

subjects were divided into four groups: less than 1 year (infant), 1 -4 years (toddler), 5 -10 years (child), and 11 -18 years (adolescents).

Exercise Testing

Normal subjects > 8 years old were also asked to perform repeated straight, alternate leg raising exercise (80-100 times) immediately after the baseline study, as described in our previous study [5]. In our present study, exercise was used as a form of increased lusitropy as proposed by Cheng et al [7].

We also tested the effect of "decreased lusitropic state" on PARR by recruiting 18 patients (mean age 9.7 years) with known clinical and echocardiographic diagnosis of dilated cardiomyopathy (DCM). From our main group of healthy subjects, we selected 30 patients matched for age, gender, and body surface area to serve as controls for the DCM group.

Echocardiography

Complete transthoracic 2DE was performed on all subjects using the commercially available iE33 ultrasound system (Philips Medical Systems, Andover, MA). Pulsed-wave Doppler was used to measure mitral valve inflow velocity, aortic outflow velocity, the timing of aortic valve closure (AVC), mitral valve opening (MVO), and isovolumic relaxation time (IVRT). Septal and lateral mitral annular tissue velocities were measured from apical views, and LV ejection fraction (EF) was measured by Simpson's method as per ASE guidelines. Short axis images of the apex at frame rates >80 Hz were obtained at the furthest apical extent of the LV cavity, just proximal to the cavity obliteration level.

Speckle-Tracking Echocardiography (STE)

STE was performed off-line by the two-dimensional Cardiac Performance Analysis software (Tom Tec Imaging Systems, Munich, Germany). Apical rotation in systole and recoil in diastole were calculated from the LV apex using STE (Figures 1 A and B). PARR was determined as the maximum value for the apical recoil rate and is represented by the tip of the sharp inflection point (blue arrow) noted in the apical recoil rate curve (Figure 1). PARR was normalized with heart rate at rest to account for differences in heart rate in this varied study population. The time sequence was normalized to percentage duration of systole, with the onset of the QRS of the ECG defined as t=0% and aortic valve closure (AVC) at end-systole, defined as t=100%. Therefore, the diastole started after 100%.

We ignored the negative signs of PARR and nPARR and utilized the absolute numerical values to describe their higher and lower values. This study was performed at the Children's Hospital of Philadelphia and is approved by its institutional review board.

Statistics

Values are expressed as mean \pm standard deviation. Paired and unpaired t-tests were used when appropriate. Linear regression analysis was performed to determine the relationship of PARR with clinical

and echocardiographic parameters. Multiple linear regression analysis was used to investigate clinical data and echocardiographic parameters that could significantly affect PARR in healthy subjects. This analysis was also used to test for independent associations between PCWP and known echocardiographic parameters of diastolic function, including e' , E/e' , and IVRT in the validation cohorts. Receiver operating characteristic (ROC) curve analyses were performed to detect cutoff values for PARR, nPARR, and IVRT to detect DD. The interobserver variability of PARR and IVRT were determined from the same stored images from 16 randomly selected patients in the validation group by 2 independent observers (AB and HK). In the DCM group, 8 patients were selected for this purpose. The intraobserver variability was measured by one observer (HK) at an interval of 14 days using stored digital images.

For all statistical analyses, a p-value < 0.05 was considered statistically significant. The statistical analysis was performed using Stata version 13. (StataCorp, College Station, TX.)

Results

Demographics and clinical characteristics

Two out of 155 healthy subjects were excluded due to poor tracing. The mean age of recruited 153 healthy subjects was 13.8 ± 2.9 years. Clinical characteristics and echocardiographic parameters are shown in Table 1.

Influence of age on Peak Apical Recoil Rate

In healthy cohorts, PARR was inversely correlated with age (Figure 2A). In infants (<1 year), the PARR values were numerically higher and dispersed further from the linear line of agreement than older children. In toddlers and older children, PARR had lower numerical values ranging from -50 to -100 %/s (Figure 2A). PARR also had a moderate association with the heart rate (Figure 2B). However, when PARR was normalized with heart rate, there was no difference in the age distribution of PARR. The average value of nPARR was -0.90 ± 0.36 %/s/min (table 1 & Figure 2C). The results from table 1 also show that time to PARR occurred before the MVO in this healthy pediatric population.

PARR was also found to have a moderate negative association with body surface area (BSA) and LV end-diastolic dimension (LVIDd) (Supplemental Figure 1). However, normalization of PARR with each of these two factors produced a strong correlation with age, suggesting that they are not effective normalizers for PARR (Supplemental Figure 2). Further analysis by multiple linear regression suggested that heart rate was the only factor that significantly affects PARR. (Table 2).

Validation cohort:

A total of 46 patients (mean age 8.5 ± 5.6 year) were evaluated, half of them had a mean PCWP of < 12 mmHg and the other half (mean age 11.3 ± 5.9 years) had a mean PCWP of ≥ 12 mmHg. The underlying cardiac diagnosis of the validation groups with normal and elevated PCWP are depicted in Table 3. The

mean filling pressure was 18.4 ± 5.6 mmHg. The clinical characteristic and findings of patients in the validation cohort are included in Table 4.

PARR and nPARR were significantly decreased in patients with elevated PCWP of ≥ 12 mm Hg, (-41.21 ± 13.37 °/s vs -87.74 ± 14.62 °/s; $p < 0.001$) and (-0.48 ± 0.12 °/s/min vs -0.98 ± 0.26 °/s/min; $p < 0.001$), respectively (Table 4 and figure 3)

Figure 4 shows ROC curves for PARR compared with IVRT, both of which were used as noninvasive predictors for PCWP ≥ 12 mm Hg, AUC: 0.98, 95% CI [0.96,1.0] vs. AUC: 0.7, 95%CI [0.54,0.86] respectively. PARR's sensitivity and specificity were noted to be excellent and superior to IVRT. A scatterplot was constructed based on the cut-off value of PARR = -52.4 °/s and nPARR = -0.66 °/s/min calculated from the ROC curves (Figure 5 A-C). PARR and nPARR demonstrated a stronger correlation to PCWP compared to IVRT ($r: 0.76$ vs. 0.2) with excellent segregation of those patients with PCWP ≥ 12 mmHg and those with normal PCWP compared with IVRT, into two distinct quadrants.

Application cohort:

a) Effect of increased lusitropy:

Fifty out of the 153 healthy subjects agreed to perform a simple exercise protocol. Two subjects were excluded due to poor tracking. PARR and nPARR increased significantly after moderate exercise compared to the resting state (-59.4 ± 19.4 °/s vs -97.82 ± 39.0 °/s, $p < 0.01$) and -0.85 ± 0.36 vs -1.4 ± 0.62 °/s/min ($p < 0.0001$). The time to PARR shortened (424.4 ± 60.3 ms vs. 322.9 ± 46.7 ms, $p < 0.0001$) (table 5)

b) Effect of decreased lusitropy:

The clinical characteristic and echocardiographic parameters of DCM patients are shown in Table 6. Two out of 18 patients were excluded because of poor tracking. PARR and nPARR were significantly lower -38.58 ± 18.59 °/s vs -63.07 ± 16.35 °/s ($p < 0.001$) and -0.43 ± 0.20 °/s/min vs -0.83 ± 0.28 °/s/min ($p < 0.0001$) respectively. The time to reach PARR was longer in DCM and occurred after the mitral valve opening.

Traditional diastolic function parameters in children with DCM

Tissue Doppler-derived septal e' and lateral e' were significantly lower with a higher E/e' ratio in the DCM group. However, no differences were noted in the mitral inflow parameters E, A, and E/A ratio. Out of 16 patients with DCM, 7 (43.7%) had a septal or lateral E/e' ratio of more than 11. Two of all DCM patients had fused E and A waves, and only one patient had reversed E/A ratio.

PARR vs. Traditional Diastolic Parameters in Predicting PCWP

PARR, average e' , E/e' and IVRT were correlated with PCWP ($r = -0.72$, $p = 0.0001$; $r = -0.3$, $p = 0.01$; $r = 0.4$, $p = 0.003$; $r = 0.2$, $p = 0.08$ respectively). Further analysis by multiple linear regression revealed that PARR

was the only significant independent variable that contributed significantly to the model ($\beta_1 = -0.19$, 95% CI: -2.74, -0.12, $p < 0.0001$). The results of multiple linear regression are shown in table 7.

Reliability

The inter-observer variability among validation cohorts, ICC coefficient for PARR and IVRT was 0.88 and 0.85, respectively, indicating good agreement between the two observers. The intra-observer correlation coefficient for PARR and IVRT was 0.95 and 0.95, respectively. In DCM patients, the ICC for intra-observer and inter-observer variability for apical recoil rate were 0.88 and 0.74, respectively.

Discussion

Current advancements in echocardiographic techniques have provided more significant insights into LV mechanics beyond the traditional measures [4]. Even though LV untwisting rate has been proposed as one of the novel indices of LV diastolic function, its use in the clinical arena has been limited due to the need for measuring recoil at apex and base separately and the need for off-line calculations [2-4]. In an elegant study using both canine and human models, Opdahl et al. have simplified the measurement of LV twist as an index of ventricular systolic function [8]. The apical rotation that occurs in the systole phase reflects the twist of the entire LV accurately and may be used as a simplified clinical index of the LV twist. However, unlike Opdahl, our focus was on early diastolic function and untwist. Therefore, we focused on the validation and application of PARR as a simplified index of LV recoil, which is an early diastolic event.

In this study, we have demonstrated that PARR reliably and accurately distinguished increased and decreased lusitropic states and may be of incremental value in evaluating early diastolic relaxation in the pediatric population. PARR is superior to IVRT and other traditional diastolic parameters (e' and E/e') in predicting elevated PCWP that can be used as an important noninvasive marker of elevated filling pressure. From a practical standpoint, correction of PARR with baseline heart rate (nPARR) caused minimal variation in nPARR values across all pediatric age groups imparting a degree of robustness that is necessary for everyday use.

Previous experimental studies have shown that a substantial portion of LV filling occurs early while the myocardium continues to relax for the first 30-40 ms after the mitral valve opening (MVO) and before the LV starts to behave as a passive structure [9]. This study showed that 21% of the stroke volume enters the LV during this phase, which has been labeled as "relaxation filling" and is related to suction. This phase is influenced by two major factors, myocardial relaxation and left atrial (LA) pressure [3]. Therefore, LV relaxation and LA pressure are intimately related. In many disease states, impaired relaxation coexists with increased myocardial stiffness. This combination typically results in increased LV filling pressure, clinically measured as elevated PCWP. Therefore, in this study, elevated PCWP was used as the gold standard for diastolic dysfunction. The conventional diastolic parameter of IVRT was chosen for comparison because PARR typically occurs before the MVO, i.e., during the isovolumic relaxation period.

In contrast, E/e' occurs later in diastole. Moreover, E/e' does not have the same reliability for detecting DD in children as compared to adults. Therefore, E/e' was not the primary focus of this study.

Peak Apical Recoil Rate as an Index of Early Diastolic Relaxation

In a canine model using tagged MRI, the influence of volume loading and pharmacologically induced increased and decreased lusitropic states on diastolic untwist during the isovolumic phase was measured [10]. Diastolic untwist rates correlated closely with the time constant of LV relaxation, τ [10]. Therefore, LV untwisting rate has evoked interest as a noninvasive index of early diastolic relaxation. Since IVRT also occurs during the relaxation phase of the diastole and is a well-established conventional index, we had chosen IVRT as an additional noninvasive index for comparison with PARR. In the canine model, IVRT has shown a fairly good correlation with the time constant of isovolumic relaxation (τ) [11]. Clinical studies in adults have also shown a good correlation of IVRT with PCWP [12]. However, in our study, the correlation of IVRT with PCWP was poor ($r=0.2$), and PARR was superior to IVRT in their correlation with PCWP. We also found that PARR is the only significant predictor of PCWP compared to the other selected traditional diastolic parameters from multiple linear regression analysis (table 7). In addition, the excellent sensitivity and specificity of PARR in detecting patients with elevated PCWP were demonstrated from the ROC curves.

Two previous studies using the canine models showed that peak untwist rate measured during isovolumic relaxation (before MVO) was not affected by increased early diastolic load [10, 13]. Because our study was clinical in nature, there was no scope for IV volume loading. Furthermore, our study in healthy subjects found that PARR was not affected by LV diameter or ejection fraction. The only clinical parameter that we found significantly influenced PARR was the heart rate. Therefore, normalization of PARR with heart rate is useful particularly in younger children. At the same time, it should be noted that based on the curve depicting age distribution of PARR (figure 2A), normalization of PARR with heart rate may not be necessary beyond eight years of age due to plateauing of the curve. A previous study in children has also demonstrated that heart rate is the primary determinant of the diastolic filling during growth [14]. Our findings are similar to a study on IVRT by Schmitz et al. that found that correction of IVRT with heart rate produced a constant value in healthy children from infants to adolescents [15].

Increased lusitropic state:

Many studies in adults have demonstrated that intraventricular pressure gradient (IVPG) increases during exercise [16]. Untwisting aids in generating this IVPG. Due to the effects of increased heart rate and sympathetic stimulation accompanying exercise, there is a more rapid fall of minimum LV pressure during isovolumic relaxation without a significant change in the left atrial pressure. It is noteworthy that infusion of dobutamine at rest also mimicked this same phenomenon [9], suggesting the usefulness of exercise in studies evaluating lusitropy in humans. The fall in early diastolic LV pressure results in an increased early diastolic pressure gradient across the mitral valve, producing an increased early diastolic LV filling rate during exercise [16]. This enhanced filling rate helps augment stroke volume despite the reduction in the diastolic duration during exercise. We found that PARR increased significantly with a

shorter duration of time to peak apical recoil in response to exercise. This increase in PARR is probably accompanied by a reduction in filling pressure and increased LV suction, allowing the enhanced filling of the ventricle within a shorter period, as demanded during exercise.

Decreased lusitropic state:

To evaluate the decrease in lusitropy, we studied a subgroup of children with a clear-cut clinical diagnosis of DCM. We found that the PARR and nPARR were significantly low. PARR occurred late at 119.5% of systole after mitral valve opening (MVO occurs at 113.5% of systole), suggesting delayed diastolic recoil in the DCM group. Our findings in normal children had demonstrated that PARR almost coincides with or just precedes MVO. These findings indicate less efficient diastolic recoil in DCM that may reduce early diastolic filling. This typically leads to a rise in LA pressure producing symptoms of exercise intolerance, such as shortness of breath [17].

Clinical implications:

Many of the noninvasive indices of DD utilized in adults are less reliable in the pediatric population. Even in adults with heart failure with preserved ejection fraction, meta-analysis studies have shown that E/e' ratio had a poor to mediocre correlation with invasive LV filling pressures [18]. The large Euro-Filling study has shown a weak correlation between single mitral inflow parameters or tissue Doppler velocities and invasive LVEDP. The average E/e' ratio had a modest correlation coefficient (r) of 0.34 with LV filling pressures [19]. In contrast, our study had found that the correlation coefficients (r) comparing PARR and nPARR with LV filling pressure were 0.7 and 0.6, respectively, which were much superior to IVRT (r=0.2), average e' (r= -0.3), and E/e' (r=0.4). Further analyses suggest that PARR is the most significant predictor for the PCWP compared to these traditional diastolic parameters. We found that the cut-off value of PARR = -52.4 °/s and nPARR = -0.66 °/s/min were excellent in detecting elevated filling pressure in children.

Limitations

In a canine model, restoring forces and LV relaxation are independent determinants of LV untwisting rate during isovolumic relaxation [13]. In these studies, restoring forces have been approximated from measurements of the systolic twist. However, this was not the focus of our study; therefore, the role of restoring forces and diastolic load on PARR was not investigated.

The 2-3-week interval between the echocardiogram and cardiac catheterization may not be ideal. However, the validation arm is a retrospective study, and in the real world, echocardiograms are often not performed simultaneously with cardiac catheterization, and many studies on children are based on such non-simultaneous data [20]. Moreover, based on available clinical records, we were reassured that the clinical state of the patients undergoing cardiac catheterization did not change during this period. Since we are proposing a new index in children, more extensive multi-center studies are needed to validate the usefulness of PARR and nPARR in the pediatric population.

Conclusion

PARR is a simplified parameter of LV untwisting with good reliability for detecting elevated LV filling pressures. PARR and nPARR are superior to IVRT in their correlation with PCWP in children and offer incremental value over other traditional indices of DD. Measurement of conventional untwist rate requires analysis of both apical and basal recoil. However, we are proposing that simply apical recoil may be sufficient. Therefore, PARR is a simplified index of LV diastolic relaxation, which may accurately reflect altered lusitropic states.

Abbreviations

PARR Peak Apical recoil rate

nPARR Normalized Peak Apical rate with heart rate

PARo Peak apical rotation

DD Diastolic Dysfunction

IVRT Isovolumic relaxation time

LV Left Ventricle

PCWP Pulmonary capillary wedge pressure

Declarations

Funding Sources: None

Disclosures: The authors declare no conflict of interest and no financial disclosures.

References

1. Dragulescu A, Mertens L, Friedberg MK (2013) Interpretation of Left Ventricular Diastolic Dysfunction in Children with Cardiomyopathy by Echocardiography Problems and Limitations. *Circ Cardiovasc Imaging* 6(2):254-61. <https://doi.org/10.1161/CIRCIMAGING.112.000175>
2. Nagueh SF, Smiseth OA, Appleton CP, Dokainish H, Edvardsen T, Flachskampf FA, et al (2016) Recommendations for the evaluation of left ventricular diastolic function by echocardiography: an update from the American Society of Echocardiography and the European Association of Cardiovascular Imaging. *Eur Heart J Cardiovasc Imaging* 4:277-314. <https://doi.org/10.1093/ehjci/jew082>
3. Burns AT, La Gerche A, Macisaac AI, Prior DL (2009) Left Ventricular Untwisting is an Important Determinant of Early Diastolic Function. *JACC Cardiovasc Imaging* 2(6):709-16.

<https://doi.org/10.1016/j.jcmg.2009.01.015>

4. Fukuda N, Terui T, Ishiwata S, Kurihara S (2010) Titin-based regulations of diastolic and systolic functions of mammalian cardiac muscle. *J Mol Cell Cardiol.* 48(5):876-881. <https://doi.org/10.1016/j.yjmcc.2009.11.013>
5. Di Maria MV, Caracciolo G, Prashker S, Sengupta PP, Banerjee A (2014) Left Ventricular Rotational Mechanics before and after exercise in Children. *J Am Soc Echocardiogr* 27(12):1336-43. <https://doi.org/10.1016/j.echo.2014.07.016>
6. Paulus WJ, Tschope C, Sanderson JE, Rusconi C, Flachskampf FA, Rademakers FE, et al (2007) How to diagnose diastolic heart failure: a consensus statement on the diagnosis of heart failure with normal left ventricular ejection fraction by the Heart Failure and Echocardiography Associations of the European Society of Cardiology. *Eur Heart J* 28:2539–50. <https://doi.org/10.1093/eurheartj/ehm037>
7. Cheng CP, Igarashi Y, Little WC (1992) Mechanism of augmented rate of left ventricular filling during exercise. *Circ Res*70(1):9-19. <https://doi.org/10.1161/01.RES.70.1.9>
8. Opdahl A, Helle-Valle T, Remme EW, Vartdal T, Pettersen E, Lunde K et al (2008) Apical rotation by speckle tracking echocardiography: a simplified bedside index of left ventricular twist. *J Am Soc Echocardiogr*21(10):1121-8. <https://doi.org/10.1016/j.echo.2008.06.012>
9. Cheng CP, Freeman GL, Santamore WP, Constantinescu MS, Little WC (1990) Effect of loading conditions, contractile state, and heart rate on early diastolic left ventricular filling in conscious dogs. *Circ Res*66(3):814-23. <https://doi.org/10.1161/01.RES.66.3.814>
10. Dong SJ, Hees PS, Siu CO, Weiss JL, Shapiro EP (2001) MRI assessment of LV relaxation by untwisting rate: a new isovolumic phase measure of tau. *Am J Physiol Heart Circ Physiol* 281(5):H2002-9. <https://doi.org/10.1152/ajpheart.2001.281.5.H2002>
11. Thomas JD, Flachskampf FA, Chen C, Guererro JL, Picard MH, Levine RA, Weyman AE (1992) Isovolumic relaxation time varies predictably with its time constant and aortic and left atrial pressures: implications for the noninvasive evaluation of ventricular relaxation. *Am Heart J* 124(5):1305-13. [https://doi.org/10.1016/0002-8703\(92\)90416-S](https://doi.org/10.1016/0002-8703(92)90416-S)
12. Appleton CP, Galloway JM, Gonzalez MS, Gaballa M, Basnight MA (1993) Estimation of left ventricular filling pressures using two-dimensional and Doppler echocardiography in adult patients with cardiac disease. Additional value of analyzing left atrial size, left atrial ejection fraction and the difference in duration of pulmonary venous and mitral flow velocity at atrial contraction. *J Am Coll Cardiol* 22(7):1972-82. [https://doi.org/10.1016/0735-1097\(93\)90787-2](https://doi.org/10.1016/0735-1097(93)90787-2)

13. Opdahl A, Remme EW, Helle-Valle T, Edvardsen T, Smiseth OA (2012) Myocardial relaxation, restoring forces, and early-diastolic load are independent determinants of left ventricular untwisting rate. *Circulation* 126(12):1441-51. <https://doi.org/10.1161/CIRCULATIONAHA.111.080861>
14. Arsos G, Moralidis E, Karatzas N, Iakovou I, Georga S, Kolioukas D, et al (2002) Heart rate is the major determinant of diastolic filling pattern during growth: a radionuclide ventriculography assessment. *Pediatr Cardiol* 23(4):378-87. <https://doi.org/10.1007/s00246-002-1506-4>
15. Schmitz L, Schneider MBE, Lange PE (2003) Isovolumic relaxation time corrected for heart rate has a constant value from infancy to adolescence. *J Am Soc Echocardiogr* 16(3):221–222. <https://doi.org/10.1067/mje.2003.17>
16. Notomi Y, Martin-Miklovic MG, Oryszak SJ, Shiota T, Deserranno D, Popovic ZB, et al (2006) Enhanced ventricular untwisting during exercise: a mechanistic manifestation of elastic recoil described by Doppler tissue imaging. *Circulation* 113(21):2524-33. <https://doi.org/10.1161/CIRCULATIONAHA.105.596502>
17. Cheng CP, Noda T, Nozawa T, Little WC (1993) Effect of heart failure on the mechanism of exercise-induced augmentation of mitral valve flow. *Circ Res* 72(4):795-806. <https://doi.org/10.1161/01.RES.72.4.795>
18. Sharifov OF, Schiros CG, Aban I, Denney TS, Gupta H (2016) Diagnostic Accuracy of Tissue Doppler Index E/e' for Evaluating Left Ventricular Filling Pressure and Diastolic Dysfunction/Heart Failure with Preserved Ejection Fraction: A Systematic Review and Meta-Analysis. *J Am Heart Assoc* 5(1):e002530. <https://doi.org/10.1161/JAHA.115.002530>
19. Lancellotti P, Galderisi M, Edvardsen T, Donal E, Goliash G, Cardim N, et al (2017) EchoDoppler estimation of left ventricular filling pressure: results of the multicentre EACVI Euro-Filling study. *Eur Heart J Cardiovasc Imaging* 18(9):961-968. <https://doi.org/10.1093/ehjci/jex067>
20. Fogel MA, Sundaeswaran KS, de Zelicourt D, Dasi LP, Pawlowski T, Rome J, Yoganathan AP (2012) Power loss and right ventricular efficiency in patients after tetralogy of Fallot repair with pulmonary insufficiency: clinical implications. *J Thorac Cardiovasc Surg* 143(6):1279-85. <https://doi.org/10.1016/j.jtcvs.2011.10.066>

Tables

Table 1: Clinical Characteristics and Echocardiographic Measurements in Normal Subjects

BSA= body surface area; SBP=systolic blood pressure; DBP=diastolic blood pressure; HR=Heart Rate; LVIDd=LV end-diastolic dimension; LVIDs=LV end-systolic dimension; PARo= Peak apical rotation; PARR= peak apical Recoil Rate; nPARR = normalized PARR with HR, Data are expressed as mean \pm SD,*P < 0.05

Variables	Less than 1 year	1 – 4years	5 – 10 years	11- < 18 years
	(Infant) (n= 29)	(Toddler) (n= 27)	(Child) (n= 39)	(Adolescent) (n= 58)
Age (yrs)	0.51±0.4	2.7±0.8*	6.8 ±1.7*	13.7±2.4*
Male	42%	46%	47%	65%
BSA (m2)	0.35±0.10	0.59±0.09*	0.90±0.17*	1.57±0.29*
SBP mmHg	92±12	99±12*	101±7*	114±11*
DBP mmHg	55± 9	60±7	58±5	63±7
HR (beats/min)	136±17	102±16*	82±13*	67±11*
E (m/s)	0.99±0.23	1.04±0.18	0.99±0.17	0.92±0.20
Septal e' (m/s)	0.11±0.03	0.12±0.02	0.13±0.02	0.14±0.02
Septal E/ e' Ratio	9.95±2.85	8.54±1.78*	7.75±1.49*	6.92±1.57*
Lateral E/ e' Ratio	7.55±2.53	6.92±1.76*	6.08±1.54*	5.37±1.20*
LVIDd (cm)	2.26±0.26	3.15±0.38*	3.78±0.35*	4.62±0.53*
LVIDs (cm)	1.39±0.23	1.96±0.24*	2.43±0.22*	2.95±0.37*
EF (%)	68±5	70±4	66±3	67±4
PARo (°)	8.81±2.26	8.14±2.66	8.13±2.02	8.75±2.67
PARR (°/s1)	-121.8± -59.8	-86.4±31.4*	-75.7±31.4*	-59.3±21.9*
nPARR (°/s/min)	-0.89±0.38	-0.86±0.36	-0.93±0.38	-0.90 ±0.36
Time to PARR as percentage of systole(%) (%)	109±13	115±16	115±14	113±11
Time to MVO as percentage of systole (%)	120 ± 3	120 ± 2	120 ± 2	119±2

Table 2. Multiple linear regression analysis with PARR as the dependent variable

Variables	Coefficients	SE	t	95% CI	P value
Age	-0.40	2.21	-0.18	-1.09- -1.28	0.85
Heart rate	-0.71	0.21	-3.34	-0.95- 0.50	0.001
Body surface area	7.8	26.3	0.30	-0.43- 0.24	0.77
LVIDd	1.26	9.78	0.06	-0.43- 0.21	0.89
Ejection Fraction	0.04	0.67	-1.162	-0.60- 0.17	0.95

R²= 0.3, adjusted R²=0.50, root mean square error = 35.7 F = 12, p < 0.0001, PARR: Peak apical recoil rate; LVIDd: LV end-diastolic dimension

Table 3. Respective cardiac diagnoses of patients with normal and elevated PCWP for validation cohort

Cardiac diagnosis	Normal PCWP	Elevated PCWP
	(< 12 mmHg)	(> 12mmHg)
	n = 23	n= 23
Restrictive cardiomyopathy	0	14
Hypertrophic Cardiomyopathy	1	6
Dilated Cardiomyopathy	0	1
Coarctation of the Aorta	3	0
Patent Ductus Arteriosus	5	0
Atrial septal defect	5	0
tetralogy of Fallot	4	0
Aortic stenosis	0	2
Kawasaki disease	1	0
Ventricular septal defect	2	0
Right ventricle myofibroma	1	0
Truncus arteriosus	1	0

PCWP: pulmonary capillary wedge pressure

Table 4. Clinical Characteristic, echocardiographic and hemodynamic data for validation cohort

Table 6: Demographic and Echocardiographic data for decreased lusitropic state produced by DCM.

Variables	All n = 46	PCWP < 12 mmHg (n=23)	PCWP ≥ 12 mmHg (n=23)	P value
Age (years) mean	8.5 ± 5.6	5.9 ± 3.87	11.3 ± 5.9	0.451
Male (%)	48	49	47	0.5
BSA (m ²)	1.06 ± 0.49	0.83 ± 0.34	1.30 ± 0.50	0.001
SBP mmHg	105 ± 16	103 ± 59	107 ± 17	0.44
Heart Rate, bpm	91 ± 24	94 ± 21	88 ± 25	0.36
Mean PCWP, mmHg	13.0 ± 6.7	7.7 ± 2.1	18.4 ± 5.6	<0.001
Mean PAP, mmHg	20.6 ± 8.9	14.3 ± 4.4	26.7 ± 8.0	<0.001
LVEF (%)	59 ± 10	63 ± 6	57 ± 11	0.1
GLS (%)	20.8 ± 2.9	21.9 ± 2.3	19.6 ± 3.0	0.005
EDSR _l	1.54 ± 0.76	2.21 ± 0.45	0.88 ± 0.33	<0.001
Average E' m/s	0.11 ± 0.05	0.14 ± 0.05	0.09 ± 0.04	0.005
Average E/e'	10.62 ± 5.96	6.38 ± 2.48	13.44 ± 6.47	<0.001
IVRT ms	55.36 ± 14.5	52.11 ± 6.61	58.61 ± 12.17	0.001
PARo (°)	8.60 ± 4.90	8.46 ± 4.26	8.73 ± 5.66	0.01
PARR (°/s)	-64.5 ± 27.0	-87.7 ± 14.6	-41.2 ± 13.4	<0.001
nPARR °/s/min	-0.73 ± 0.32	-0.98 ± 0.26	-0.48 ± 0.12	<0.001
Time to PARR (ms)	395 ± 78	376 ± 58	415 ± 93	0.09
Time to PARR as percentage of systole (%)	121.5 ± 13.3	122.2 ± 12.9	130.4 ± 14.2	0.320
MVO as percentage of systole (%)	118.8 ± 8.4	116.3 ± 5.5	124.9 ± 10.1	0.045

BSA: Body Surface Area; SBP: Systolic blood pressure; PCWP: pulmonary capillary wedge pressure; PAP: Pulmonary artery pressure; IVRT: isovolumic relaxation time; PARo: Peak apical rotation; PARR: Peak apical recoil rate; nPARR: normalized peak apical recoil rate; MVO mitral valve opening; GLS: global longitudinal strain; EDSR: longitudinal early diastolic strain rate; Data are expressed as mean ± SD

Table 5. Peak Apical Recoil Rate in Normal Subjects in Response to exercise

Variables	Rest	Exercise	P value
	n = 48	n= 48	
Peak Apical Rotation (°)	7.70 + 2.70	9.70 ± 5.47	< 0.05
Peak Apical Recoil Rate(°/s)	-59.4 ± 19.4	-97.8 ± 39.0	<0.01
Normalized Peak Recoil Rate by HR (°/s/min)	-0.85 ± 0.34	-1.4 ± 0.62	<0.0001
Time to Peak Apical Recoil rate (ms)	424 ±60	322 ± 47	< 0.0001
Apical Recoil Slope (°/s)	-37.3 ± 15.5	-64.6 ± 27.4	< 0.0001

Variables	Control (n=32)	Dilated Cardiomyopathy (n=16)	P value
Age (years)	10.1±5.6	9.7 ± 6.3	0.83
Male (%)	50	50	1
BSA (m ²)	1.4 ±0.7	1.1± 0.6	0.28
Heart Rate	83.4 ±24.3	92.3 ± 22.7	0.23
LVIDd (cm)	4.0 ± 0.9	4.6 ± 0.9	0.03
LVIDs (cm)	2.49 ±0.56	3.49±0.87	< 0.00001
FS (%)	37.6 ±3.8	25.3 ± 8.5	< 0.00001
EF(%)	67.6 ±5.4	48.1 ± 13.6	<0.00001
E velocity (m/s)	0.91 ± 0.25	0.97 ± 0.33	0.47
A velocity (m/s)	0.52 ± 0.21	0.57 ± 0.20	0.44
E/A	1.9 ± 0.64	1.85 ± 0.73	0.23
Septal e' (m/s)	0.13 ± 0.02	0.09 ± 0.02	<0.0001
Lateral e' (m/s)	0.18 ± 0.04	0.11 ± 0.04	<0.0001
Septal E/e'	6.80 ± 2.90	11.29 ± 6.02	<0.001
Lateral E/e'	5.26 ± 2.07	10.07 ± 6.18	0.0003
DT (ms)	191.6 ± 55.3	211.9 ± 64.4	0.27
Peak Apical Rotation (°)	7.88 ± 2.64	5.33 ± 2.65	0.0029
Peak Apical Recoil Rate (°/s)	-63.07±16.35	- 38.58 ± 18.59	<0.0001
nPARR °/s/min	-0.83 ± 0.28	-0.43 ± 0.20	<0.0001
Time to PARR (ms)	395 ± 63	398 ±76	0.90
Time to PARR as percentage of systole (%)	116.5 ±17.9	119.5 ± 18.8	0.59
MVO as percentage of systole (%)	117.7 ± 5.9	113.7 ± 5.8	0.02

BSA=Body surface area; LVIDd=LV end-diastolic dimension; LVIDs=LV end-systolic dimension; FS=Fraction shortening; EF=Ejection Fraction, DT=Deceleration Time. Data are expressed as mean ±SD, PARR= peak apical recoil rate, nPARR: normalized peak apical recoil rate

Table 7. Multiple linear regression analysis with PCWP as the dependent variable

Variables	Coefficients	SE	t	95% CI	P value
PARR (%/s)	-0.19	0.03	-5.07	-0.27, -0.12	0.0001
IVRT	-0.05	0.08	-0.67	-0.21 , 0.11	0.51
Average e'	-0.89	3.96	-0.22	-8.90 ,7.11	0.8
E/e'	-0.07	0.18	-0.39	-0.43, 0.29	0.7

$R^2 = 0.55$, adjusted $R^2 = 0.49$, root mean square error = 4.9, $F = 9.4$ $p < 0.0001$, PARR: Peak apical recoil rate; IVRT: isovolumic relaxation time

Figures

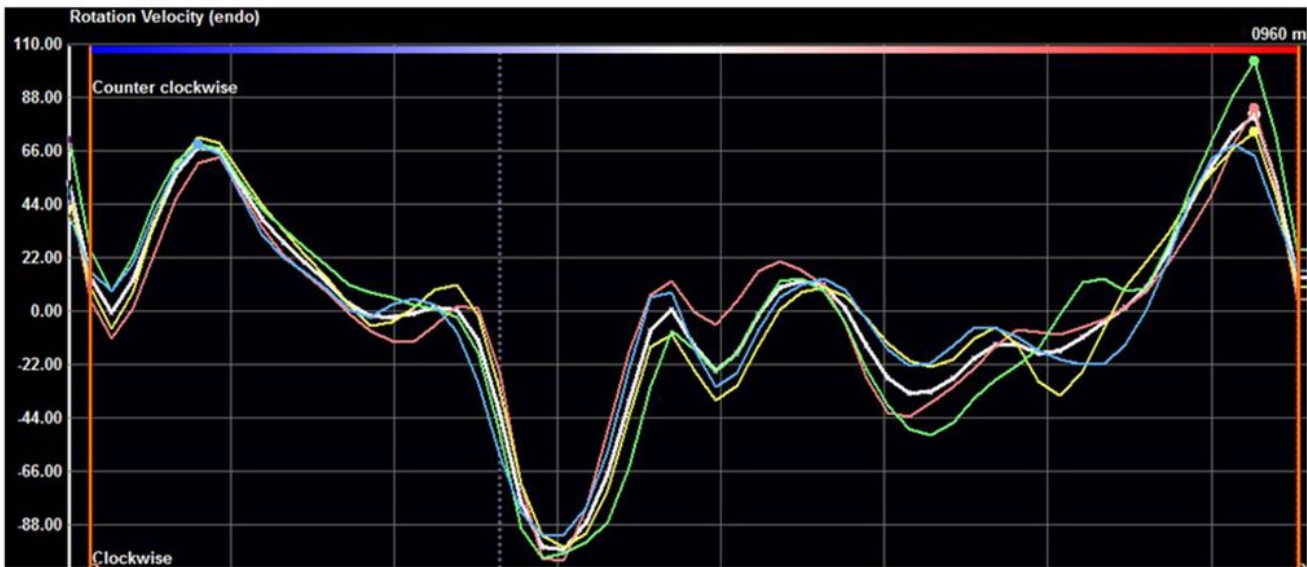
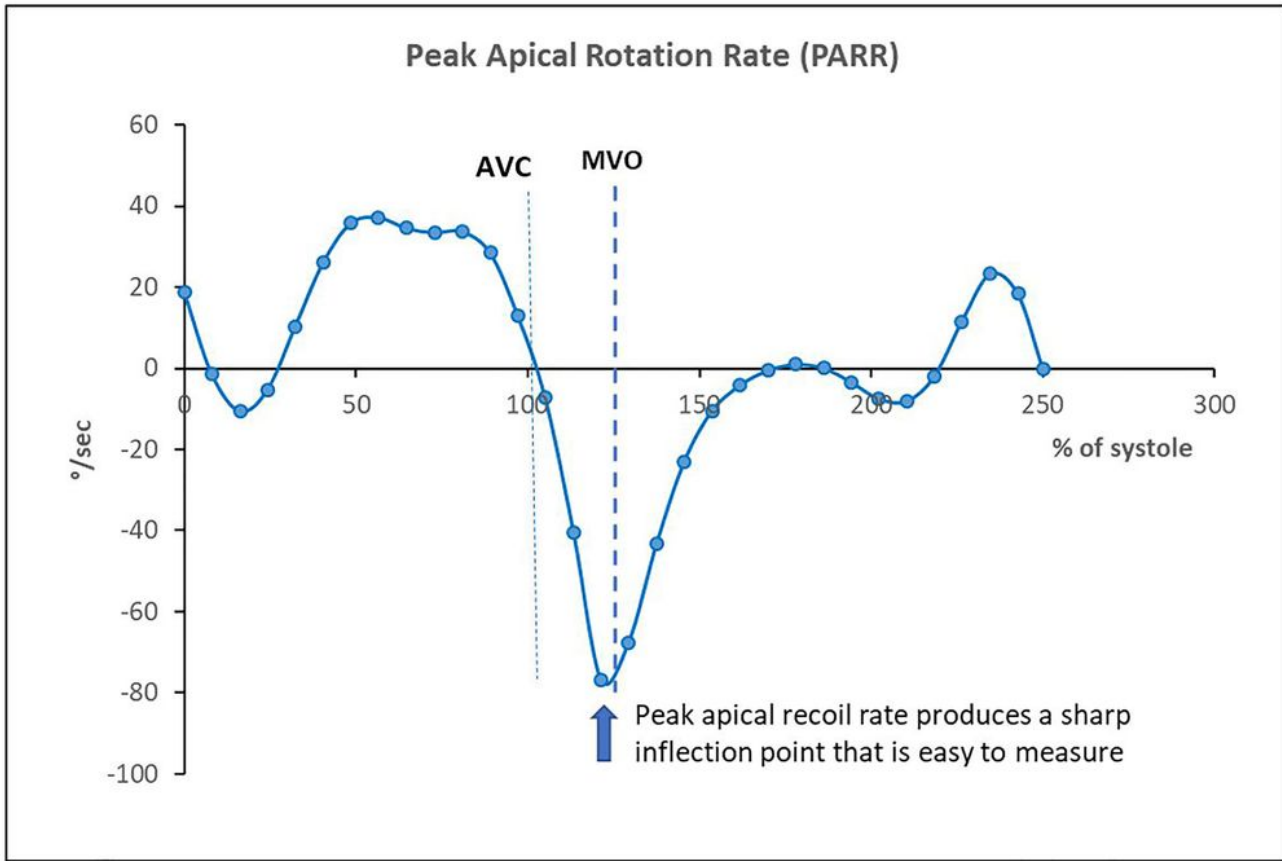


Figure 1

A. The peak apical recoil rate (PARR) is the maximum value for the apical recoil rate and is represented by the tip of the prominent inflection point (blue arrow). The peak inflection typically occurs just before the mitral valve opening (MVO). B. Typical wave forms derived from speckle tracking imaging from LV apex using Tom Tec imaging software. The cardiac cycle was measured between two QRS waves of the ECG, and ED frames are represented by the vertical red lines.

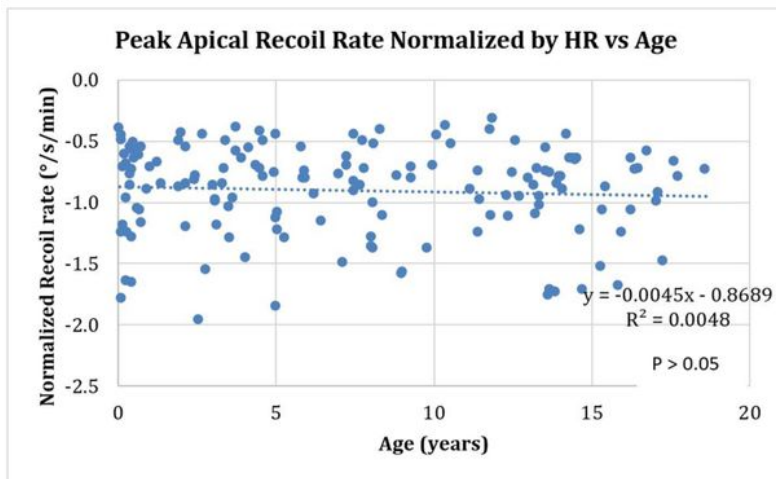
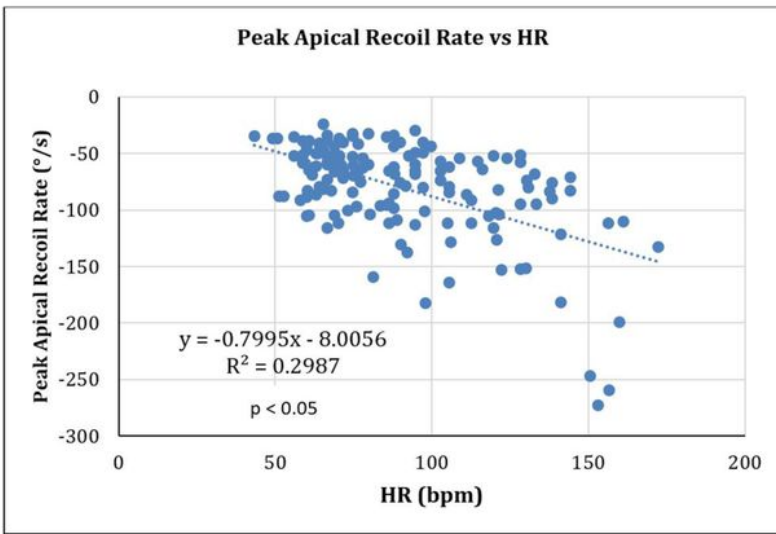
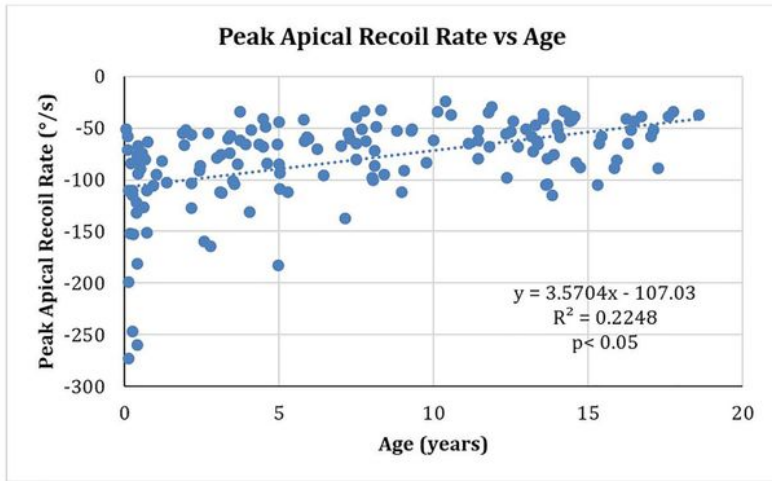


Figure 2

A: A graph describing the relationship of PARR and patient age. The PARR values in younger infants were more negative and disperse from the linear line compare with older children. B: A graph describing the relationship between PARR and heart rate. PARR had a negative association with the heart rate, showing that as heart rate increased, PARR decreased. It is notable that since PARR is a negative value, the magnitude of PARR increases with heart rate. C: A graph describing the relationship between Age and

PARR normalized by heart rate (nPARR), showing no significant difference in nPARR across the pediatric group.

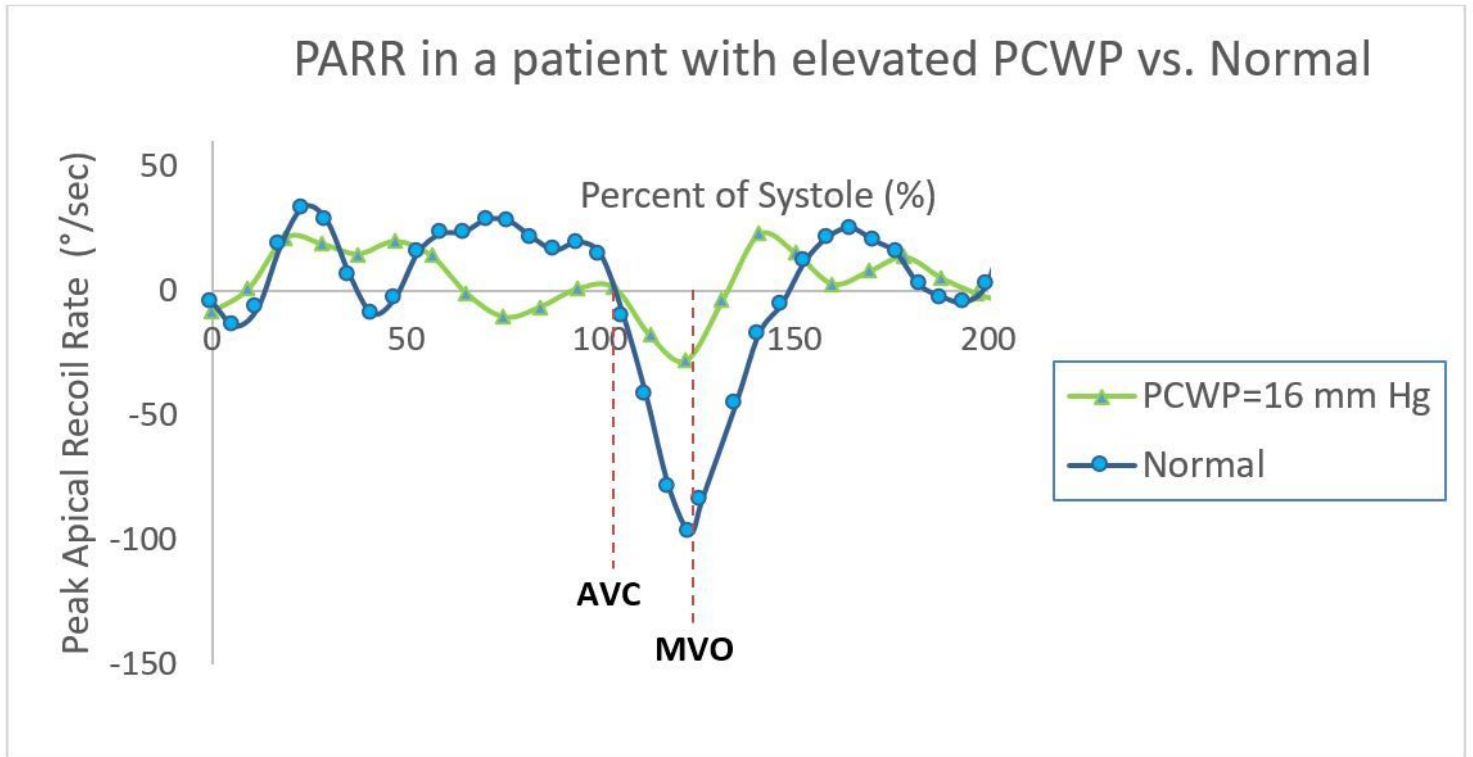


Figure 3

Representative waveforms depicting apical recoil rate for a healthy child versus a patient with elevated PCWP. Aortic valve closure (AVC) times for both normal and elevated PCWP patients are marked by the vertical dashed line (100% systole) and at mitral valve opening (MVO).

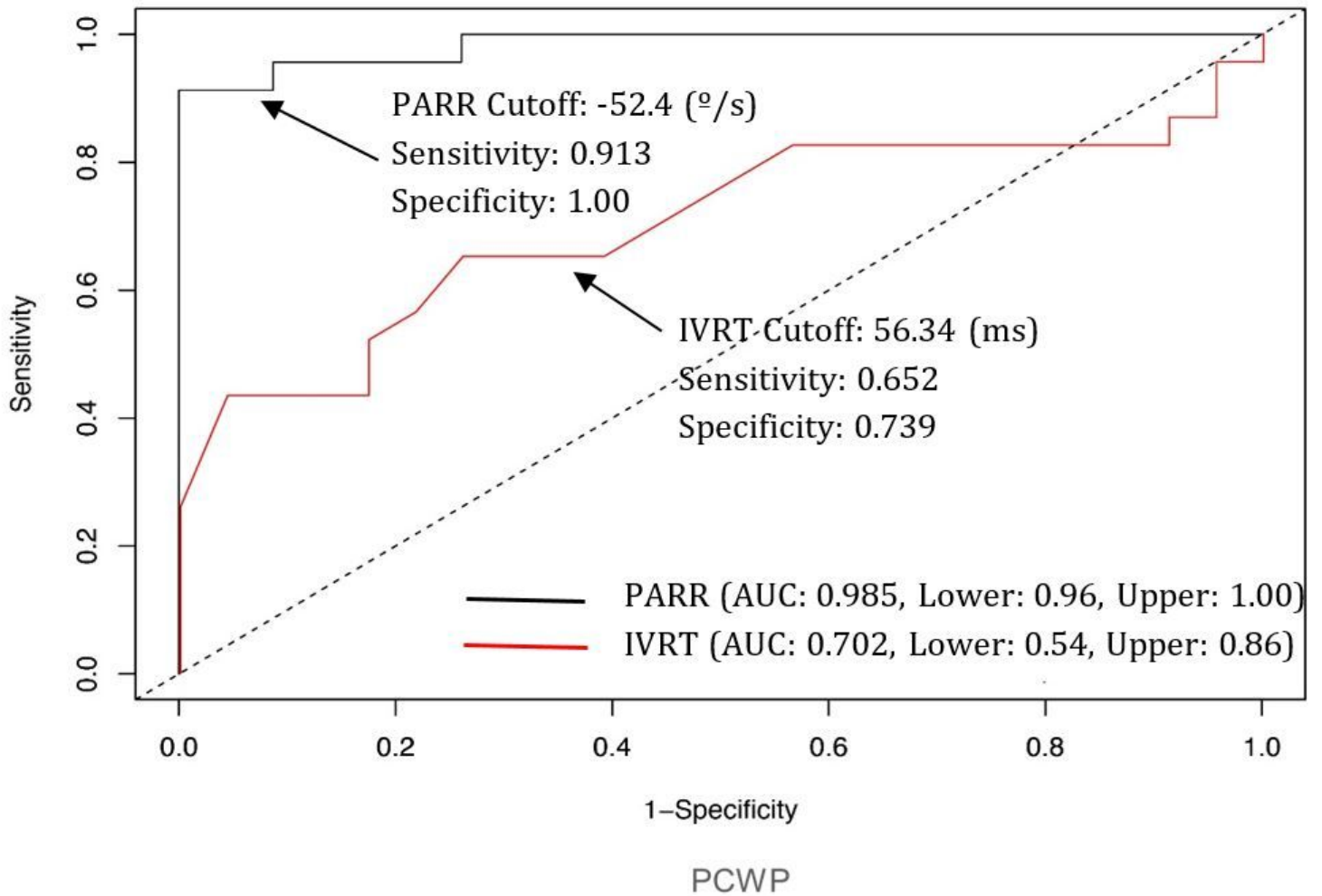


Figure 4

ROC curves showing PARR is superior to IVRT with excellent sensitivity and specificity in detecting patient with elevated PCWP

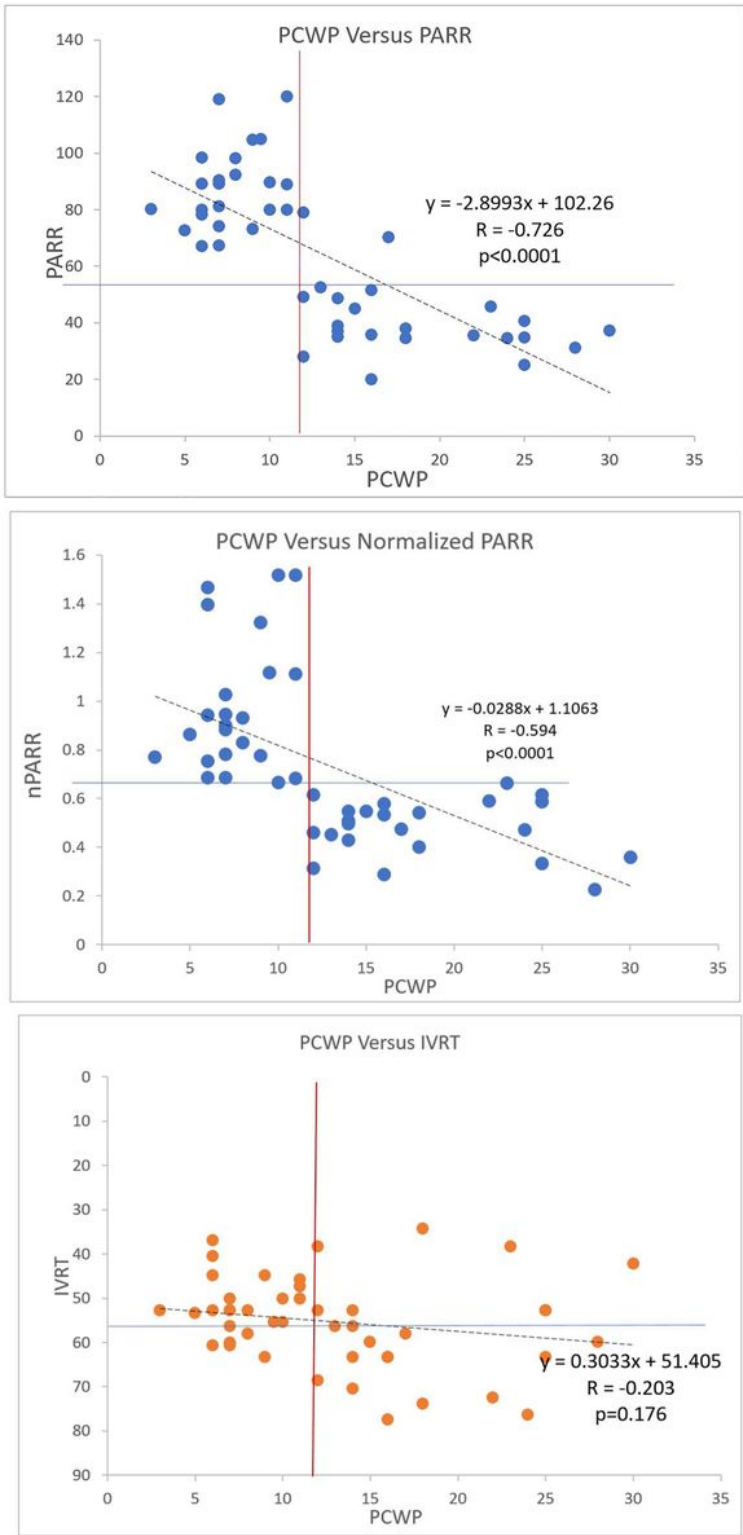


Figure 5

Correlation of PCWP with PARR (A) nPARR (B) and IVRT(C). PARR and nPARR shows superior correlation with PCWP than IVRT. This is characterized by tight segregation of data in the “north-west” and “south-east” quadrants. The blue horizontal lines represent the cutoff values for PARR and nPARR described by ROC analysis. The red vertical lines are positioned at PCWP=12, the cutoff value describing elevated PCWP in this study.

Supplementary Files

This is a list of supplementary files associated with this preprint. Click to download.

- [SupplementalFigures.docx](#)